JOURNAL OF CATALYSIS 104, 331–338 (1987)

Physicochemical Properties of a Delaminated Clay Cracking Catalyst

MARIO L. OCCELLI,*[,1] STEVEN D. LANDAU,†[,2] AND THOMAS J. PINNAVAIA†[,3]

* *Gulf Research and Development Company, P.O. Drawer 2038, Pittsburgh, Pennsylvania 15230, and*
† *Department of Chemistry, Center for Fundamental Materials Research, Michigan State University, East Lansing, Michigan 48824*

Received May 28, 1986; revised November 18, 1986

A delaminated clay cracking catalyst, formed by reaction of Na^+ Laponite with an aluminum chlorohydrate solution, has been examined with regard to thermal stability, pore size distribution, and other catalytically relevant properties. The previously proposed card house structure, wherein edge–face layer aggregation competes favorably with face–face aggregation, is compatable with the observed physicochemical properties. Thermal analysis and N_2 adsorption measurements indicate that the delaminated structure is retained up to ~600°C. Heating above 600°C results in the nearly complete collapse of the delaminated structure at 730°C, the formation of enstatite ($MgSiO_3$), spinel, and quartz at 900°C, and the generation of more spinel ($MgAl_2O_4$) and crystobalite near 1100°C. The N_2 and *n*-pentane adsorption isotherms (Type II) fit the BET equation, as expected for a macroporous structure. The pore size distributions derived from N_2 adsorption data, along with pore distributions obtained by Hg intrusion, show that the delaminated clay does, in fact, consist mainly of macroporosity, qualitatively similar to an amorphous aluminosilicate catalyst containing 22 wt% Al_2O_3. This result is in contrast to the regular microporosity typical of alumina pillared clays with well-ordered face–face lamellar structures. Finally, temperature-dependet IR studies of chemisorbed pyridine on delaminated Laponite indicate that the surface acidity is mainly of the Lewis type.

Pinnavaia *et al.* (1–3) have recently demonstrated that the flocculation of smectite clays by polyoxocations can lead to delaminated aggregates when the layer lateral dimensions are small (≤0.05 μm) or the layer morphology is lathlike. Under these latter conditions edge–face layer association competes favorably with face–face association. A "card house" structure has been proposed for delaminated clays which differs dramatically from the well-ordered face–face lamellar structures formed by pillared clays when the layer size is large (≤2 μm) and pancakelike in morphology (aspect ratio ~10^3). Delaminated structures are favored by the small particle size fraction of trioctahedral hectorite or, better, by the synthetic hectorite analog Laponite. The more commonly observed lamellar structures are typified by pillared derivatives of montmorillonite and beidellite.

Delaminated clays exchanged with polyoxocations exhibit acid catalytic properties (*4*) comparable to those of pillared clays. For instance, equivalent yields of light cycle gas oil are obtained for the cracking of gas oil by delaminated and pillared clays at 515°C. Although the reactivities of delaminated and pillared clays are similar, delaminated clays exhibit much greater macroporosity than pillared clays. Their improved carbon selectivity in cracking, for example, is attributed to their moderate acidity and their macroporosity which favors desorption of high-molecular-weight hydrocarbons which otherwise would be retained as coke (*5*). Enhanced macroporosity also could be an advantage in catalytic reaction systems where mass transfer is an important kinetic consideration.

In the present work we examine the porosity and other catalytically related prop-

[1] Present address: Unocal Corp., P.O. Box 76, Brea, CA 92621.

[2] Present address: U.S. Industrial Chemicals, 1275 Section Rd., Cincinnati, OH 45241.

[3] To whom all correspondence should be addressed.

0021-9517/87 $3.00

erties of a delaminated clay formed by the reaction of Na^+ Laponite with aluminum chlorohydrate (ACH) in aqueous solution. ACH solutions have been previously shown (*1–6*) to contain Keggin-like polyoxocations of the type $Al_{13}O_4(OH)_{24+x}(H_2O)_{12-x}^{(7-x)+}$. These Al_{13} oligomers bind readily to clay surfaces by ion exchange (*7–9*) and impart catalytically useful Brønsted and Lewis acidity (*4, 5, 10–13*) when dehydrated at elevated temperatures. The results reported here for delaminated Laponite are compared with those for an ACH pillared montmorillonite and an amorphous aluminosilicate cracking catalyst, AAA-alumina.

EXPERIMENTAL

The delaminated clay catalyst used in this work was prepared by reaction of a synthetic hectorite, Laponite (Laporte Industries, Ltd.), with an aluminum chlorohydrate solution (Chlorhydrol, Reheis Chemical Co.) according to procedures described elsewhere (*1*). The pillared clay catalyst, an ACH pillared montmorillonite, was prepared according to previously described procedures (*6*). The amorphous silica–alumina catalyst (78% SiO_2, 22% Al_2O_3), designated AAA-alumina, was obtained from American Cyanamid.

A Digisorb 2600 from Micromeritics Instrument Corporation was used to measure N_2 sorption, BET surface areas, and pore size distributions. Mercury penetration porosimetry measurements were performed using a Quantachrome porosimeter. Differential thermal analyses (DTA) and thermal gravimetric analyses (TGA) were obtained with a DuPont 1090 thermogravimetric analyzer using heating rates of 20 and 10°C/min, respectively. Nitrogen (50 cm^3/min) was used as a purge gas; the sample weight was ~10 mg. Infrared (IR) spectra were obtained with a DuPont 1100 spectrometer. Self-supporting wafers were prepared by pressing 8-mg samples on a die 10 mm in diameter for 1 min at ~10,000 lb under vacuum. Prior to pyridine sorption, the wafers were mounted in an optical cell and degassed by heating at 400°C for 10 h at 10^{-6} Torr. The pyridine-loaded wafers were then heated *in vacuo* in the 25–500°C temperature range for a period of 1 h and the spectra recorded for each temperature. Scanning electron micrographs (SEM) were taken with a JEOL JSM-35 instrument.

RESULTS AND DISCUSSION

The thermal properties of an X-ray amorphous delaminated Laponite are shown by the TGA, DTA, and N_2 BET surface area (SA) curves shown in Fig. 1. A sample initially equilibrated in air under ambient conditions exhibits a cumulative weight loss of ~16.0 wt% over the temperature range 25–700°C. An additional 1.7 wt% is lost between 700 and 1100°C and an inflection point is found between 700 and 800°C. The weight loss below 700°C is attributed mainly to the loss of residual pore water and to the dehydration/dehyroxylation of the surface-bound aluminum cations.

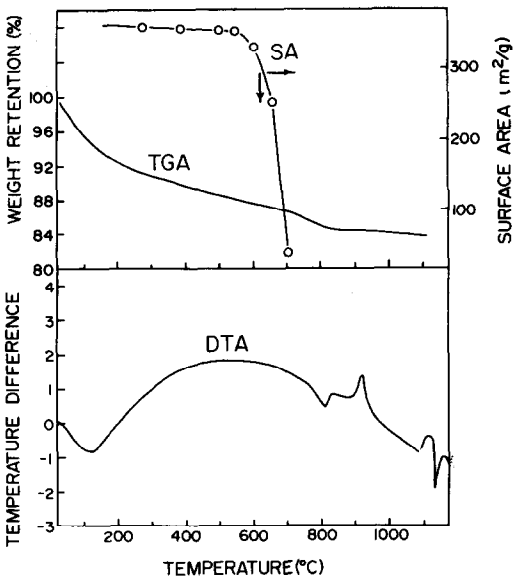

FIG. 1. Thermal gravimetric analysis (TGA) and differential thermal analysis (DTA) curves for delaminated Laponite. Also shown is the dependence of the N_2 BET surface areas (SA) on dehydration temperature (6 h heating time).

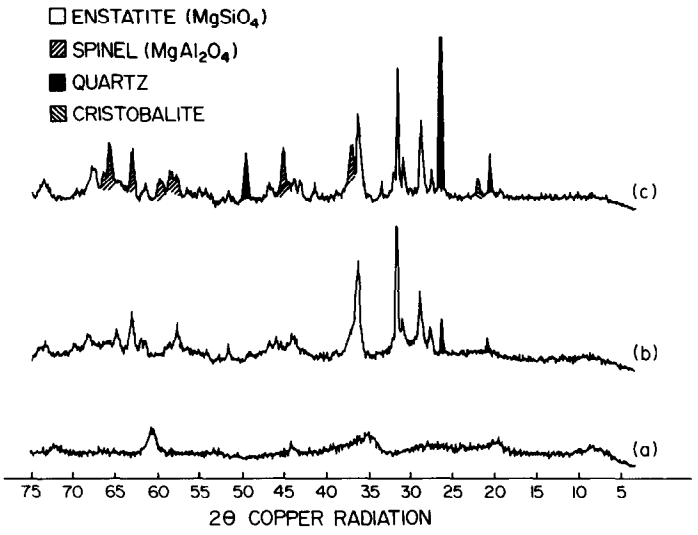

FIG. 2. X-ray powder diffraction patterns (Cu$K\alpha$) of delaminated Laponite after calcination in air for 2 h at (a) 400°C, (b) 950°C, and (c) 1100°C.

The loss of water below 700°C is accompanied by a very broad endotherm in the DTA curve. Also, the inflection point which occurs at 700–800°C in the TGA curve is accompanied by a relatively sharp endotherm. Two additional thermal processes are revealed in the DTA curve near 900 and 1100°C.

The X-ray powder diffraction patterns show that the initial delaminated Laponite is essentially X-ray amorphous. As shown by the diffraction pattern in Fig. 2a, heating to 400°C for 2 h results in the appearance of broad diffraction lines which may reflect partial collapse of the delaminated structure and some face–face layer ordering ($d_{001} \simeq 9$–10 Å). That the delaminated structure is lost by 600°C is demonstrated by the temperature dependence of the N_2 BET surface area shown in Fig. 1. In the range 300–600°C there is only a 10% decrease in the surface area from the initial value of 384 m^2/g. Above 600°C, however, the surface area decreases dramatically, and collapse of the structure is essentially complete by 730°C, where the surface area is reduced to $\simeq 25$ m^2/g.

The thermal transition which occurs at 700–800°C is not accompanied by the formation of a new crystalline phase. Thus, the latter transition may represent the dehydroxylation of the clay layer and/or the reaction of the surface aluminum cations with the silicate sheet of the 2:1 layer structure. However, the exothermic transition near 900°C results in the formation of enstatite ($MgSiO_3$) along with some spinel and high-temperature quartz, as represented by the powder diffraction pattern in Fig. 2b. The more thermally complex reaction near 1100°C affords more spinel ($MgAl_2O_4$) and the transformation of some quartz into cristobalite.

Figure 3 shows SEMs of delaminated Laponite before and after heating in air at 960 and 1100°C for 2 h. Before heating, the particles appear as glassy shards. After heating, the sharp edges are lost, apparently due to incipient sintering.

Nitrogen and *n*-pentane adsorption isotherms for delaminated Laponite are compared in Fig. 4 with those for an amorphous aluminosilicate (AAA-alumina) and a typical pillared montmorillonite. On the basis of the shapes of the adsorption isotherms up to intermediate partial pressures (Type II),

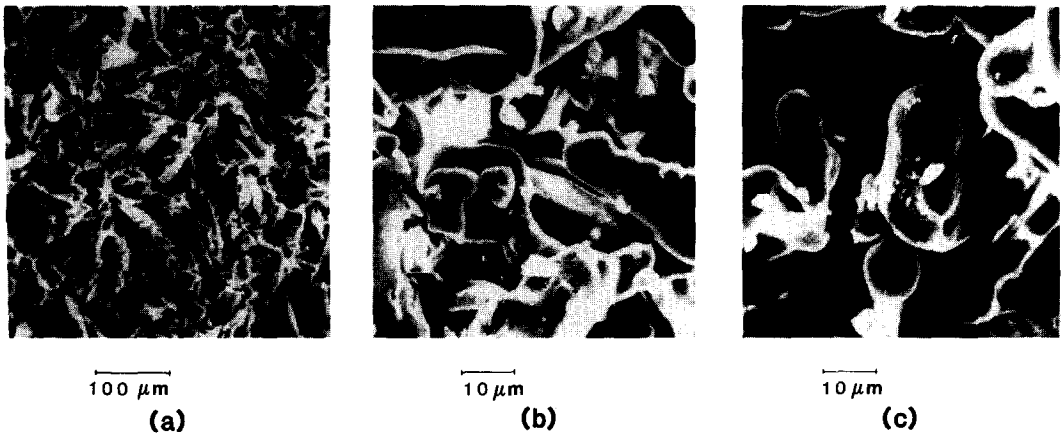

FIG. 3. SEMs of delaminated Laponite after calcination at (a) 400°C, (b) 950°C, and (c) 1100°C.

the delaminated clay and AAA-alumina catalyst exhibit multilayer adsorption behavior. However, the pillared clay exhibits zeolite-like Type I behavior, as expected for a regular, microporous material.

As shown in Figs. 5 and 6, the BET equation provides satisfactory linear fits of the N_2 and *n*-pentane adsorption data for delaminated Laponite and AAA-alumina, whereas the Langmuir equation does not. For the pillared montmorillonite, however, the Langmuir equation provides a slightly better fit of the adsorption data than the BET equation, the correlation coefficients lying in the range 0.997–0.999. Langmuir-type isotherms also have been observed previously for pillared montmorillonite (*14, 15*).

Incremental pore volume and pore area distributions for delaminated Laponite, as determined from the N_2 adsorption isotherms, are compared in Figs. 7 and 8 with

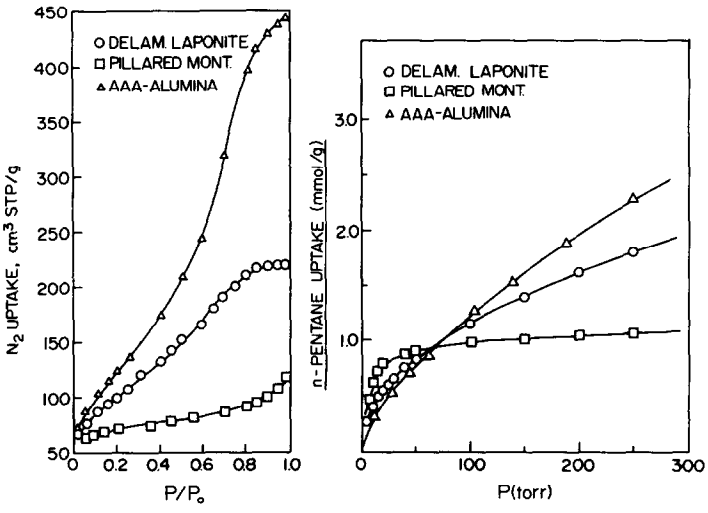

FIG. 4. A comparison of nitrogen adsorption isotherms (−196°C, left) and *n*-pentane adsorption isotherms (25°C, right) for delaminated Laponite, pillared montmorillonite, and amorphous aluminosilicate (AAA-alumina).

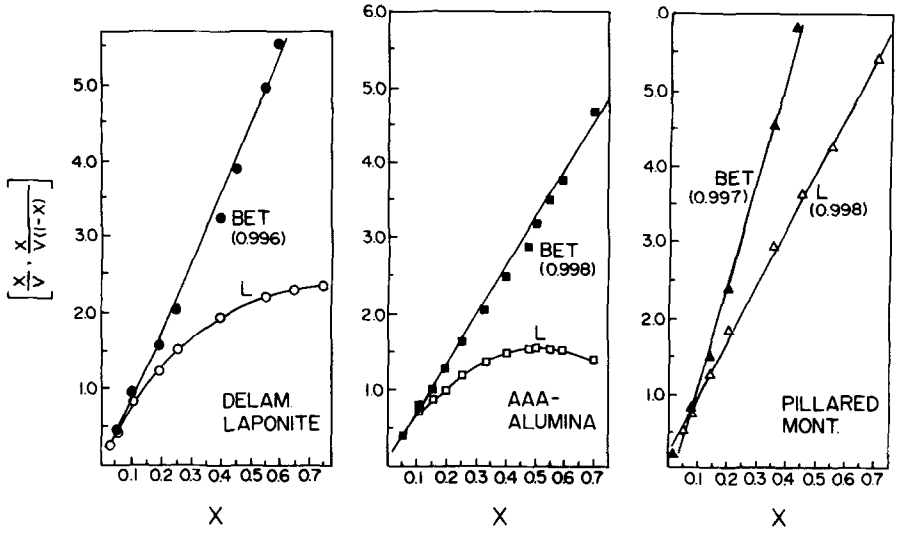

FIG. 5. Nitrogen adsorption data plotted according to the Langmuir equation (X/V vs X) and BET equation ($X/[V(1 - X)]$ vs X), where $X = P/P_0$. Values in parentheses are correlation coefficients obtained by linear regression analysis.

those for the AAA-alumina and pillared montmorillonite. The pore distributions of the delaminated clay more nearly approximate those of the amorphous aluminosilicate than the pillared clay (*1–3*). The delaminated clay has 50% of the N_2 surface area (384 m^2/g) in pores >30 Å diameter, compared with 47% for the amorphous silica–aluminum. In contrast, only 20% of the N_2 surface area of the pillared clay arises from pores >30 Å diameter. Thus, the delaminated clay possesses less microporosity than the pillared clay. These results are in agreement with the originally proposed card house structures for a delaminated clay and a face–face lamellar structure for a well-ordered pillared clay.

The existence of macropores in delaminated Laponite is readily demonstrated by high-pressure Hg intrusion measurements

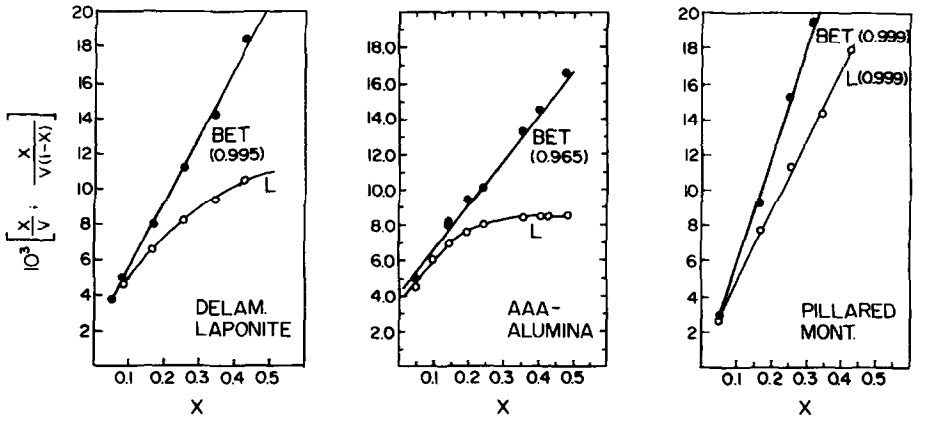

FIG. 6. *n*-Pentane adsorption data plotted according to the BET and Langmuir adsorption isotherms. Values in parentheses are correlation coefficients obtained by linear regression analysis.

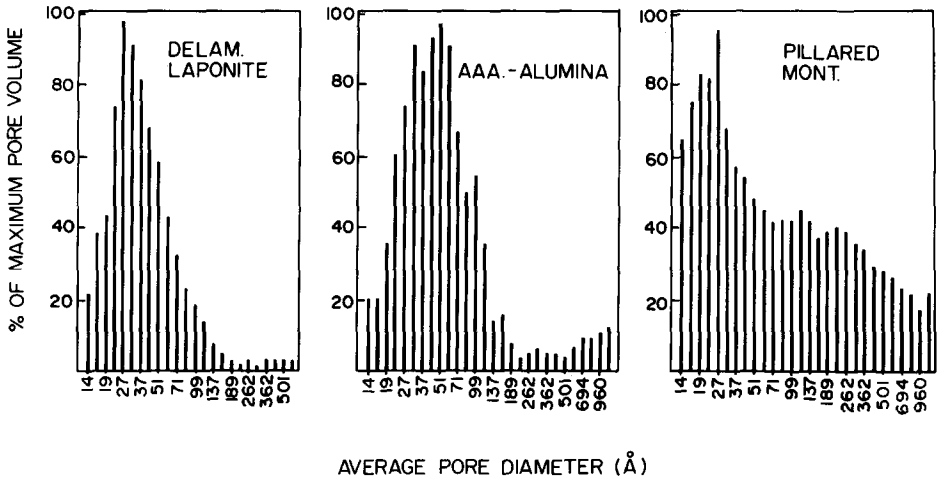

FIG. 7. Pore volume distributions determined from the N_2 adsorption data.

(60,000 psi). In order to obtain greater resolution of the pore distribution in the macroporous range, we also have carried out low-pressure Hg intrusion measurements (0–1200 psi). The results of the low-pressure measurement are summarized in Table 1. These data show that 50% of the Hg pore volume (0.22 cm^3/g) of the delaminated clay results from pores ≥100,000 Å. Pores >15,000 Å diameter account for 90% of the void volume. The corresponding volume fraction–pore diameter relationships for AAA-alumina, are 50% ≥3600 Å and 90% ≥950 Å. Thus, the structure of the delaminated clay results in a much broader macropore distribution than AAA-alumina. For pillared montmorillonite, the macroporous volume arises from pores which are intermediate between the delaminated clay and the amorphous silica–alumina. Macroporosity in pillared clays may be formed by layer folding and by the generation of void volume between tactoid particles.

Table 2 compares the absolute values of

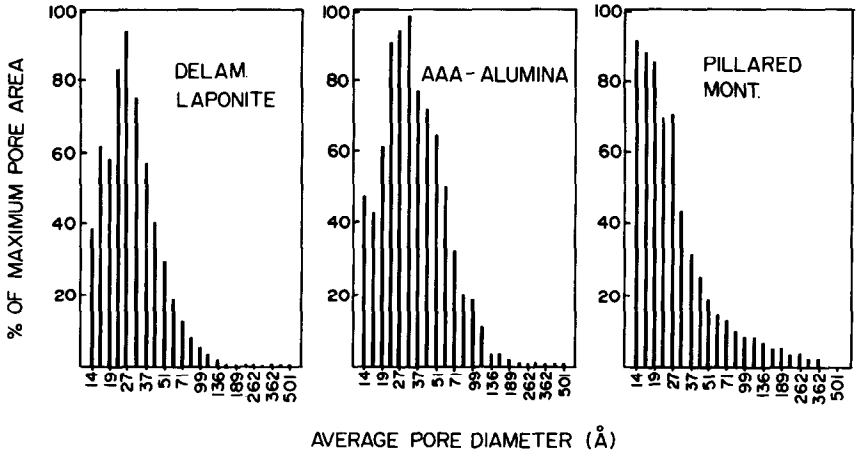

FIG. 8, Pore area distributions determined from the N_2 adsorption data.

TABLE 1

Pore Size Distributions Obtained from Low-Pressure (0–1200 psia) Mercury Porosimetry Measurements

Volume % in given pore radius range	Pore radius (Å)		
	Delaminated clay	Pillared bentonite	AAA-alumina
10	500,000	240,000	39,000
30	200,000	78,000	7,900
50	100,000	32,000	3,600
70	56,000	12,000	1,500
90	15,000	2,800	900

TABLE 2

Pore Volumes (V) and Pore Surface Areas (Å) Obtained from Hg Intrusion Measurements at 1200 and 60,000 psi

Catalyst	1200 psia		60,000 psia	
	V (cm^3/g)	Å (m^2/g)	V (cm^3/g)	Å (m^2/g)
Delaminated Laponite	0.20	0.21	0.24	33.7
Pillared montmorillonite	0.24	0.58	0.36	2.7
AAA-alumina	0.21	1.3	0.55	190.0

the pore volumes and pore areas obtained by Hg intrusion at 1200 and 60,000 psi. For the delaminated clay, the Hg pore volume (0.20 cm^3/g) is lower than the N_2 pore volume (0.35 cm^3/g). The pore areas for the delaminated clay and AAA-alumina increase dramatically upon increasing the intrusion pressure, as expected for solids with broad pore size distributions. In contrast, the pore area of a well-ordered pillared clay is much less sensitive to Hg pressure due to the inaccessibility of the microporous structure at 60,000 psi.

Infrared studies of adsorbed pyridine have been useful as a means of probing the surface acidity of pillared clays (*16*). Montmorillonites pillared by alumina typically exhibit both Bronsted and Lewis acidity under ambient conditions. However, at temperatures which more nearly approximate cracking conditions (400°C), the pyridine is retained primarily on Lewis acid sites. The presence of Lewis acidity suggests that the high activity of pillared clays for gas oil cracking may involve a hydride abstraction mechanism, as suggested for other cracking catalysts with Lewis acidity (*17*). Thus, it was of interest in the present work to qualitatively compare the pyridine adsorption properties of delaminated Laponite and pillared montmorillonite.

Pyridine was adsorbed onto a pressed wafer of delaminated Laponite which had been previously calcined in air at 400° for 4 hr. Figure 9 illustrates the infrared absorption spectra obtained after heating the pyridine-loaded wafer at various temperatures under vacuum (10^{-6} Torr). The spectrum at 28°C exhibits bands at 1450, 1492, 1579, and 1618 cm^{-1} which are characteristic of pyridine bound to Lewis acid sites. These latter

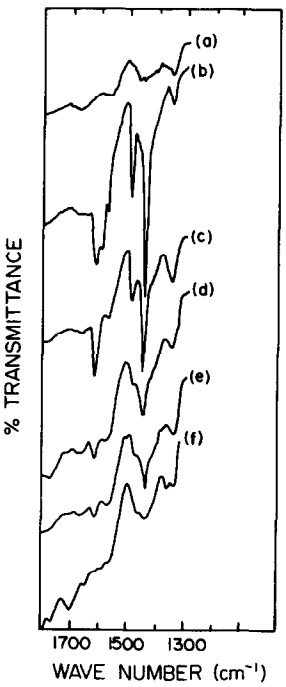

FIG. 9. Infrared absorption spectra of (a) delaminated Laponite after having been heated under vacuum at 400° and of pyridine retained on this delaminated Laponite after heating in vacuum to (b) 28°C, (c) 200°C, (d) 300°C, (e) 400°C, and (f) 500°C for 1 h at each temperature.

sites are presumed to be coordinatively unsaturated aluminum centers on the surface bound alumina. The band at 1600 cm^{-1} is attributed to physically adsorbed pyridine. Significantly, there is no clear evidence for a 1540-cm^{-1} band which would indicate the presence of Brønsted acidity. Thus the surface acidity appears to be mainly of the Lewis type.

Heating the pyridine-loaded delaminated clay results in the loss of the physically adsorbed species below 200°C. At 400°C, most of the chemisorbed pyridine is lost. Under comparable conditions, a well-ordered pillared montmorillonite would retain significantly more pyridine. Thus the Lewis acid strength of delaminated Laponite is somewhat less than a compositionally analogous pillared montmorillonite. The origin of the Lewis acidity differences between delaminated and pillared clays remains to be investigated.

ACKNOWLEDGMENTS

M.L.O. wishes to thank Ms. Alice Cavanaugh (DOE, Pittsburgh) for technical assistance and Drs. D. Finseth and S. S. Pollack (DOE, Pittsburgh) for many helpful discussions. S.D.L. and T.J.P. acknowledge support of this research by the National Science Foundation (DMR/8514154), the Michigan State University Center for Fundamental Materials Research, and the Environmental Protection Agency.

REFERENCES

1. Pinnavaia, T. J., Tzou, M. S., Landau, S. D., and Raythatha, R. H., *J. Mol. Catal.* **27,** 195 (1984).
2. Pinnavaia, T. J., *in* "Heterogeneous Catalysis" (B. L. Shapiro, Ed.), pp. 142–164. Texas A&M Univ. Press, College Station, 1984.
3. Pinnavaia, T. J., *in* "Chemical Reactions in Organic and Inorganic Constrained Systems" (R. Setton, Ed.), pp. 151–164. Reidel, Dordrecht, 1986.
4. Occelli, M. L., Landau, S. D., and Pinnavaia, T. J., *J. Catal.* **90,** 256 (1984).
5. Occelli, M. L., and Lester, J. E., *Ind. Eng. Chem. Prod. Res. Dev.* **24,** 27 (1985).
6. Akitt, J. W., and Farthing, A., *J. Magn. Reson.* **32,** 345 (1978).
7. Plee, D., Borg, F., Gantineau, L., and Fripiat, J. J., *J. Amer. Chem. Soc.* **107,** 2362 (1985).
8. Diddams, P. A., Thomas, J. M., Jones, W., Ballantine, J. A., and Purnell, J. H., *J. Chem. Soc. Chem. Commun.*, p. 1340 (1984).
9. Pinnavaia, T. J., Landau, S. D., Tzou, M.-S., and Johnson, I. D., *J. Amer. Chem. Soc.* **107,** 7222 (1985).
10. Lussier, R. J., Magee, J. S., and Vaughan, D. E. W., *in* "7th Canadian Symposium on Catalysis, Edmonton, Alberta, Canada, October 19–22, 1980" preprint.
11. Shabtai, J., Lazar, R., and Oblad, A. G., *New Horiz. Catal.* **1,** 828 (1981).
12. Occelli, M. L., *in* "Proceedings, 8th International Clay Conference, Denver, CO," in press.
13. Kibuchi, E., Matsuda, T., Fujika, H., and Morita, Y., *Appl. Catal.* **11,** 331 (1984).
14. Yamanaka, S., and Brindley, G. W., *Clays Clay Miner.* **27,** 119 (1979).
15. Occelli, M. L., Parulekar, V., and Hightower, J., *in* "Proceedings 8th International Congress on Catalysis Berlin, 1984," Part IV, p. 725.
16. Occelli, M. L., and Tindwa, R. M., *Clays Clay Miner.* **31,** 22 (1983).
17. Venuto, P. B., and Habib, E. T., "Fluid Catalytic Cracking with Zeolite Catalyst." Dekker, New York, 1979.